PRE-TEST PREDICTION AND POST-TEST ANALYSIS OF PWR FUEL ROD BALLOONING IN THE MT-3 IN-PILE LOCA SIMULATION EXPERIMENT IN THE NRU REACTOR

A.T. DONALDSON, R.A. HORWOOD, T. HEALEY
Central Electricity Generating Board,
Berkeley Nuclear Laboratories,
Berkeley, Gloucestershire,
United Kingdom

SYNOPSIS

The USNRC and the UKAEA have jointly funded a series of in-pile LOCA simulation experiments in the Canadian NRU reactor in order to secure further information on the thermal hydraulic and clad deformation response of PWR fuel rod bundles. Test MT-3 in the series was performed using reflood rate and rod internal pressure conditions specified by the UK nuclear industry. The parameters were selected to ensure the development of a near-isothermal clad temperature history during which zircaloy was required to balloon and rupture near the alpha-alpha/beta phase transition. Specification of the reflood rate conditions was assisted by the performance of a precursor test on an unpressurised rod bundle and by complementary application of appropriate thermal hydraulic analyses. Identification of the rod internal pressure needed to cause ballooning and rupture was achieved using a creep deformation model, BALLOON, in conjunction with the clad thermal history defined by the prior thermal hydraulic test. This paper presents the basis of the BALLOON analysis and describes its application in calculating the fill gas pressure for rods MT-3, their axial ballooning profile and the clad temperature at peak radial strain elevations.

1. INTRODUCTION

The ballooning response of PWR fuel rods under postulated LOCA conditions has been the subject of intensive investigation during the past ten years. Experimental studies have included numerous out-of-pile and in-reactor tests on single rods and a smaller number of multi-rod experiments in out-of-pile facilities. To complement the latter work, a programme of in-reactor experiments on PWR fuel bundles was initiated by the Fuel Behaviour Research Branch of the United States Nuclear Regulatory Commission in conjunction with Pacific Northwest Laboratories. The major objectives of the project were to evaluate the thermal-hydraulic and mechanical deformation response of a full length PWR fuel bundle during the heat-up, reflood and quench phases of a LOCA. The facility selected

for the test programme was the Canadian NRU reactor at Chalk River Nuclear Laboratory operated by the Atomic Energy of Canada.

The United Kingdom Atomic Energy Authority has contributed to the NRU programme on the basis that the UK industry would specify the test conditions for one of the experiments in the series. In particular, attention was focussed on the ballooning response of rods subjected to near-isothermal conditions in the high alpha phase temperature range during reflood. To support the UK experiment, thermal-hydraulic analyses and clad creep deformation studies were undertaken. The former work indicated that the desired transient would be attained by varying the reflood rate and this was subsequently confirmed by precursor experiments on unpressurised fuel bundles in the NRU reactor.

To assist identification of the rod fill pressure needed to promote ballooning, mechanical property tests on NRU fuel cladding were also performed in conjunction with complementary creep modelling calculations. This paper summarises the work undertaken in support of the latter task, which has resulted in the development of a clad deformation model, BALLOON. Application of the model to assist evaluation of the fill gas pressure for the MT-3 rods is described and a comparison of the predicted and observed axial ballooning profiles is presented. It is shown that the average clad temperature of the peak ballooning regions can be evaluated from a knowledge of the measured clad temperature in the vicinity of peak strain regions, the rod pressure variation during ballooning and the steady state creep behaviour of zircaloy.

2. THE FUEL ROD DEFORMATION MODEL

2.1 Initial Geometry

The fuel rod configuration for the in-pile tests in the NRU reactor is illustrated in Figure 1. To determine the axial ballooning profile of a 'nominal' fuel tube it is sub-divided into 29 nodes each five inches long. Radial dilation of the nodes is unrestricted but no axial deformation is permitted. Within each node, clad dilation is presumed to occur at constant metal volume and to remain uniform over the node length. Support grids are located at intervals along the length of the rods and are assumed to prevent local clad ballooning.

2.2 Input Parameters

The driving force for ballooning arises from the helium fill gas pressure in the fuel rods. In a closed system, the hot pressure of the fixed mass of gas varies as the tube expands and its internal volume increases. To predict the ballooning response of the cladding it is

necessary to define;

(i) the initial tube length, diameter and wall thickness.

(ii) the initial total internal free volume of the fuel rod and its axial distribution.

(iii) the initial fill gas pressure at known volume and temperature.

(iv) the correlation between the instantaneous fill gas pressure and stress in the tube wall.

(v) the relationship between clad deformation rate and instantaneous stresses and temperature.

(vi) the thermal history of both the fill gas and the cladding.

The initial tube dimensions and the distribution of gas free volume in each of the 29 axial nodes are defined by the rod design parameters. These are summarised in Table 1. The initial fill gas pressure is a variable parameter and for the present study, calculations were performed using values equal to 430, 500 and 530 psi.

Tube ballooning was presumed to occur entirely by secondary creep in response to a hoop stress related to the instantaneous tube dimensions and internal pressure. The general creep equation for NRU zircaloy fuel cladding was determined in a parallel investigation[7]

The clad thermal history measured during a preceding thermal hydraulics test using unpressurised pins (TH - 2.14) was identified as a model transient for the MT-3 ballooning experiment [2]. The thermocouple output from several rods at various axial levels, Figure 2, was used to construct a clad temperature profile for a 'nominal' rod undergoing the transient. The temperature-time-axial location array, interpolated from the thermocouple data, is shown in Table 2. The temperature-time history measured at axial levels 13 and 15 is compared for the TH2.14 test and the actual MT-3 experiment in Figures 3 and 4.

The filling gas temperature was presumed to be related to the instantaneous clad temperature. The effect on ballooning of gas temperatures equal to the instantaneous clad temperature T_c, and $T_c - 20^\circ$, 40° and 60°C respectively was examined.

2.3 Creep Deformation Analysis

Gas mass flow rates within the fuel tube assembly are assumed to be sufficiently rapid to maintain a homogeneous equilibrium pressure in the tube throughout a temperature transient. The pressure, P_g, in the fuel tube can therefore be calculated for any axial temperature profile and axial free

volume distribution from the relation

$$\frac{P_o V_o}{T_o} = P_E \sum_{1}^{29} \left(\frac{V_i}{T_i}\right) \qquad (1)$$

where P_o is the cold fill pressure, V_o the total gas free volume at the filling temperature T_o; V_i and T_i are the free volume and mean gas temperature respectively in each axial node.

The clad axial temperature distribution varies with time during a transient and in the present calculation has been specified by the temperature-time-axial location array shown in Table 2.

The original gas free volume per axial node, $(V_i)_o$, is known, and the original tube internal volume per node, $(V_T)_o$, is given by the relation

$$(V_T)_o = \frac{\pi}{4} (d_o - 2t_o)^2 L_o \qquad (2)$$

where d_o, t_o and L_o are the tube outer diameter, wall thickness and node length respectively. The residual volume per node, V_K occupied by fuel, thermocouples and other instruments is given by differences as:

$$V_K = (V_T)_o - (V_i)_o \qquad (3)$$

This volume is assumed to remain invariant throughout the transient. It follows that the gas volume per node, $(V_i)_t$, at any time during the transient is

$$(V_i)_t = (V_T)_t - V_K \qquad (4)$$

where $(V_T)_t$ is the instantaneous tube volume per node, given by the relation

$$(V_T)_t = \frac{\pi}{4} (d_i - 2 t_i)^2 L_o \qquad (5)$$

The terms d_i and t_i are the instantaneous diameter and wall thickness and L_o is the unchanged node length.

Both d_i and t_i can be expressed in terms of the original tube dimensions, and the mid-wall diametral engineering strain, e, by the relations

$$\begin{aligned} d_i &= (d_o - t_o)(1 + e) + t_o (1 + e)^{-1} \\ t_i &= t_o (1 + e)^{-1} \end{aligned} \qquad (6)$$

Furthermore, the engineering strain, e, and true strain, ε, are related according to the expression

$$\varepsilon = \log_e (1 + e) \qquad (7)$$

whilst the true strain $(\varepsilon)_i$ in a given node at any time, t, during a transient is given by the integral

$$(\varepsilon)_i = \int_0^t \dot{\varepsilon}_i \, dt \qquad (8)$$

where $\dot{\varepsilon}_i$ is the instantaneous hoop strain rate and depends on the hoop stress, σ and the temperature T according to the expression [2]

$$\dot{\varepsilon}_i = A \left(\frac{G}{E}\right) \left(\frac{\sigma}{G}\right)^n \exp - \frac{Q_i}{RT} \qquad (9)$$

For the zircaloy-4 cladding used in the present series of NNU tests,

the structure constant $A = 6.54 \times 10^{16}$ N^{-1} m^2 K sec^{-1}

the stress exponent $n = 4.94 \pm 0.09$

and the activation energy $Q_i = 294.0 \pm 16.0$ Kj $mole^{-1}$

The elastic shear modulus G ($N\ m^{-2}$) is given by

$$G = 3.326 \times 10^{10} - 2.244 \times 10^{7} (T - 273) + 2.161 \times 10^{3} (T - 273)^2$$

and R has its usual meaning.

The integral in equation 8 may be solved by numerical iteration using the expressions

$$(\varepsilon)_i = \Sigma \Delta\varepsilon_i \qquad (10)$$

and $$\Delta\varepsilon_i = \dot{\varepsilon}_i \, \Delta t \qquad (11)$$

providing the time step, Δt, is sufficiently small for the strain rate, $\dot{\varepsilon}_i$, to remain constant during the interval. Equation 9 may then be used to determine the appropriate strain rate, $\dot{\varepsilon}_i$, since the variation of temperature, T_i, with time is known, Table 2. The hoop stress, σ_i in a given node may be calculated from the expression

$$\sigma_i = \frac{P_g (d_i - t_i)}{2 t_i} \qquad (12)$$

where P_g is the current equilibrium gas pressure and is determined by equation 1.

The preceding deformation analysis which forms the basis of the BALLOON model commences by calculating the equilibrium pressure at the start of the transient for the specified initial temperature profile and initial gas volume distribution. The initial hoop stress in each of the axial nodes along the fuel rod is evaluated using the initial rod dimensions. Initial strain rate and strain increment are calculated and

the new tube volume after the first time step is recalculated together with the new gas volume. The new temperature profile is then imposed and a new equilibrium pressure is calculated. The iteration loop is repeated to determine the stress for the new node dimensions, and hence the new strain rate, strain, tube dimensions and gas volume. The entire calculation is repeated until the node with the largest strain has doubled its initial diameter when rupture is deemed to occur.

3. PREDICTED BALLOONING RESPONSE AND ROD PRESSURE SELECTION

3.1 Near-Isothermal Conditions

The preceding model was used to evaluate the ballooning response of the 'nominal' rod in the MT-3 bundle when subjected to the thermal transient described in Table 2. The analysis was performed to establish the effect of rod fill gas pressures equal to 450, 500 and 550 psi on the axial ballooning profile and time-to-rupture. The predicted variation of maximum tube diameter and hot gas pressure as a function of the cold fill pressure for the clad thermal history described in Table 2 is shown in Table 3 and Figures 5a - c. As the initial cold fill pressure was increased from 450 to 550 psi, the calculated time to rupture decreased from a value in excess of 170 seconds to less than 100 seconds depending on the assumed hot gas temperature.

The calculated axial ballooning profiles are shown in Figures 6 to 8 for assumed gas temperatures equal to the clad temperature T_c, and in excess of T_c by 60°C. Cold fill pressures of 450, 500 and 550 psi were again selected and comparison of the Figures shows that ballooning was predicted to occur over three grid spans for each pressure history. In all cases, the maximum radial strain was located at level 15 (node 20 - 21) whilst smaller strain peaks occurred at levels 13 and 17 corresponding to nodes 16 and 24.

3.2 Adiabatic Heating

The model was also used to examine the effect on rupture temperature of maintaining a clad thermal ramp of 8°C sec^{-1} which corresponded to the adiabatic heating rate prior to reflood. For this calculation, it was assumed that the cladding experienced an axial thermal history identical to that defined in Table 2 for the period up to 40 seconds. Temperatures at levels 13 to 17 (nodes 16 to 24) were then allowed to rise at 8°C sec^{-1} (see Figures 3 and 4) whilst the remaining nodes maintained the temperature history specified in Table 2. Clad failure was predicted to occur appreciably earlier but at a higher temperature than calculated for the transient conditions defined by Table 2. Thus, for a cold fill pressure of 550 psi and a clad-to-gas temperature difference of 60°C, the calculated rupture time was 51 seconds which corresponded to a rupture temperature of 860°C. The small margin of 11 seconds between the occurrence of rupture during uncontrolled adiabatic heating and the required temperature turn-round time of 40 seconds

to near-isothermal heating emphasised the need for precise control of the reflood rate parameters in the MT-3 test.

3.3 Rod Pressure Selection

An essential requirement of the MT-3 test was that rod-to-rod interaction should occur during the reflood phase of the near-isothermal transient. On the basis of the previous calculations, a cold fill pressure of 550 psi was selected for each of the twelve MT-3 rods. For a clad thermal transient identical to that defined by the precursor thermal hydraulic experiment, this pressure was predicted to promote ballooning strains in excess of 0.1 and 0.3 above level 13 and 15 respectively after approximately 100 seconds. Application of the lower pressure of 450 psi was predicted to require near isothermal heating in excess of 170 seconds to promote ballooning and rupture. In order to ensure adequate deformation during the thermal transient, but to minimise the risk of premature failure during adiabatic heating, the reflood parameters were modified for MT-3 to ensure earlier turn-over of the initial heat-up rate. Subsequent performance of the MT-3 experiment demonstrated that the required thermal conditions were attained at levels 13 and 15, Figures 3 and 4.

4. DISCUSSION

4.1 Comparison of Model Predictions with Experiment

Application of the creep deformation model, BALLOON, to predict the rod fill pressure requirements for any ballooning experiment is dependent on the prior availability of information describing the axial temperature history of the cladding. Such data were provided by the precursor thermal hydraulic experiment on an identical fuel bundle containing unpressurised rods. The introduction of fill gas pressures between 450 and 550 psi into rods sustaining such a transient was calculated to promote rod ballooning for which the predicted axial profiles are shown in Figures 6 to 8. Comparison of the predicted profiles with the typical measured ballooning response of rods in the MT-3 test, Figure 9, illustrates that there is good agreement in three important respects. First, the calculated response was characterised by the development of three strain peaks occupying adjacent intergrid spans in the vicinity of levels 13, 15 and 17. This is consistent with the observed profiles in the MT-3 test. Second, tube rupture was observed to occur towards the top of the intergrid span above level 15 at a height of 105 inches; the calculated location of the rupture zone was 100 inches. Finally, the observed mean strains at the peak deformation zones above levels 13 and 17 were respectively 0.13 and 0.02. These values are consistent with the model predictions of 0.11 and 0.01 respectively.

The levels of agreement between prediction and observation lends confidence to the use of the creep deformation model as an analysis tool for further calculations of the ballooning response of MT-3 rods. Thus, one rod (2C), containing thermocouples at levels 13 and 15 was also attached to a transducer which recorded the rod internal pressure variation up to rupture[3] Since the pressure history was defined, deformation of a single axial position could be examined in isolation provided its thermal history was known. For rod 2C, the measured pressure history, Figure 10, may be used in conjunction with the equations 8 to 12 to calculate the diametral strains at levels 13 and 15 for their respective temperature histories. Such a calculation predicts large strains at level 13 and rupture at level 15 within 114 seconds. In fact, rod 2C did not rupture until ∿ 122 seconds into the reflood transient. However, the pressure transducer on the same rod indicated an internal pressure of ∿ 150 psi after rupture although the containment pressure was ∿ 40 psi, Figure 10. It was assumed that this difference corresponded to a fixed zero error, ΔP, which persisted throughout the MT-3 transient. On this basis, the true internal pressure, P_{TRUE}, was related to the observed pressure, P_{OBS}, according to:

$$P_{TRUE} = P_{OBS} - \Delta P$$

The effect of transducer zero errors, in the range $100 \leq \Delta P \leq 200$ psi, on the strains predicted at levels 13 and 15 after 122 seconds was examined. A value of ΔP equal to 150 psi enabled the best agreement with the observed strains to be obtained and was in reasonable accord with a post-calibrated transducer zero error of 75 psi.

Clad temperature thermocouples were not located on the peak radial strain regions in rod 2C corresponding to axial elevations of 84 and 103 inches. Furthermore, no record of their temperature history during deformation was obtained. However, by assuming that

$$\left.\begin{aligned} T_{103} &= T_{97} + K_{103} \\ \text{and} \quad T_{84} &= T_{76} + K_{84} \end{aligned}\right\} \text{ for } P = 150$$

it was possible to perform strain calculations for various values of K_{103} and K_{84} until $\epsilon_{103}/\epsilon_{97}$ and $\epsilon_{84}/\epsilon_{76}$ matched those observed in MT-3. On this basis, the temperature at the peak strain position (103 inches) exceeded that measured at level 15 (97 inches) by 16°C whilst the temperature calculated at the 84 inch elevation exceeded the measured value at level 13 (76 inches) by 54°C. The larger temperature difference required to match the respective strains at the lower axial positions possibly reflects the close proximity of

the rising quench front to these locations during the latter stages of the MT-3 transient.

5. CONCLUSIONS

5.1 The deformation model, BALLOON, correctly predicts the occurrence of three axial strain peaks in the MT-3 rods. The calculated position of rupture and the relative peak strain heights are also in good agreement with observations.

5.2 The predicted rupture time depends on the initial fill gas pressure and on the relation assumed between the gas and clad temperatures. The range of rupture times ($100 \leq t_r \leq 170$ seconds) determined from the calculations brackets the experimental values.

5.3 The close agreement between model prediction and experiment lends confidence to the use of the creep model for additional analysis on instrumented fuel rods. In this respect radial strain matching between level 13 (76 inches) and the adjacent peak strain position for rod 2C (84 inches) requires a temperature enhancement of 54°C. At the higher level of 103 inches, development of the observed strain profile requires the maintenance of a temperature differential of 16°C above that experienced at 97 inches.

ACKNOWLEDGEMENT

This paper is published by permission of the Central Electricity Generating Board.

REFERENCES

[1] Donaldson, A.T., Horwood, R.A. and Healey, T. Central Electricity Generating Board Report TPRD/B/0007/N82 and "Water Reactor Fuel Element Performance Modelling", Preston, England, March 1982.

[2] Mohr, C. "Thermal Hydraulic Test No. 2 LOCA Simulation in NRU Reactor", NUREG/CR/2526 and Pacific Northwest Laboratory Report PNL 4164.

[3] Mohr, C. "Materials Test No. 3 LOCA Simulation in the NRU Reactor", NUREG/CR/2528 and Pacific Northwest Laboratory Report PNL 4166.

TABLE 1 : NRU Fuel Rod Internal Gas Volume and Tube Dimensions

Axial Nodes	Gas Volume per Node (cm^3)
1 - 3	0.65
4	0.58
5 - 13	0.30
14	0.33
15 - 22	0.39
23 - 27	0.48
28	1.53
29	7.82
	Total 20.43

Tube Outside Diameter 9.65 mm

Tube Wall Thickness 0.58 mm

TABLE 2

Axial Variation of Clad Temperature as a Function of Time into Transient

[illegible]	[illegible]

[illegible]

TABLE 3

Variation of Maximum Tube Diameter and Hot Gas Pressure as a Function of Cold Fill Pressure and Time into Transient

	COLD FILL PRESSURE PO=3.1 MPa (450 psi)								COLD FILL PRESSURE PO=3.45 MPa (500 psi)								COLD FILL PRESSURE 3.79 MPa (550 psi)							
KO(C)	0		20		40		60		0		20		40		60		0		20		40		60	
Time Into Transient sec	Dmax cm	Phot MPa	Dmax cm	Phot MPa	Dmax cm	Phot MPa	Dmax cm	Phot MPa	Dmax cm	Phot MPa	Dmax cm	Phot MPa	Dmax cm	Phot MPa	Dmax cm	Phot MPa	Dmax cm	Phot MPa	Dmax cm	Phot MPa	Dmax cm	Phot MPa	Dmax cm	Phot MPa
10	9.65	6.95	9.65	7.17	9.65	7.38	9.65	7.6	9.65	7.72	9.65	7.96	9.65	8.21	9.65	8.44	9.65	8.69	9.65	8.76	9.65	9.03	9.65	9.29
20	9.65	7.1	9.65	7.32	9.65	7.54	9.65	7.76	9.65	7.89	9.65	8.14	9.65	8.38	9.65	8.62	9.65	8.68	9.65	8.95	9.65	9.22	9.65	9.49
30	9.653	7.1	9.653	7.33	9.653	7.56	9.654	7.78	9.654	7.89	9.655	8.14	9.656	8.39	9.657	8.64	9.657	8.67	9.658	8.95	9.659	9.23	9.661	9.5
40	9.678	7.01	9.682	7.24	9.688	7.47	9.694	7.69	9.697	7.77	9.705	8.02	9.714	8.26	9.724	8.51	9.725	8.51	9.738	8.78	9.753	9.04	9.77	9.29
50	9.73	6.4	9.745	6.62	9.761	6.84	9.78	7.05	9.785	7.05	9.811	7.28	9.839	7.5	9.872	7.71	9.87	7.65	9.911	7.88	9.958	8.1	10.012	8.3
60	9.788	6.03	9.815	6.23	9.846	6.43	9.881	6.61	9.886	6.59	9.933	6.79	9.987	6.98	10.049	7.15	10.039	7.09	10.118	7.27	10.211	7.43	10.319	7.57
70	9.836	5.41	9.874	5.61	9.918	5.79	9.969	5.96	9.971	5.89	10.036	6.08	10.118	6.25	10.21	6.4	10.186	6.3	10.306	6.46	10.45	6.59	10.625	6.69
80	9.889	5.26	9.941	5.45	10.001	5.62	10.071	5.77	10.067	5.7	10.162	5.87	10.274	6.01	10.409	6.13	10.363	6.04	10.54	6.16	10.761	6.25	11.045	6.3
90	9.906	5.21	10.063	5.37	10.155	5.51	10.264	5.63	10.25	5.59	10.398	5.71	10.581	5.8	10.81	5.87	10.719	5.83	11.032	5.88	11.446	5.88	12.122	5.81
100	10.157	5.21	10.281	5.33	10.433	5.43	10.619	5.5	10.59	5.49	10.856	5.54	11.281	5.55	11.781	5.51	11.506	5.55	12.301	5.45	13.962	5.22	TR<	100
110	10.341	4.95	10.523	5.04	10.754	5.1	11.053	5.13	11.006	5.13	11.471	5.11	12.197	5.03	13.621	4.81	12.994	4.93	TR<	112	TR<	104	-	-
120	10.452	4.77	10.681	4.84	10.975	4.88	11.376	4.87	11.309	4.87	11.987	4.81	13.305	4.61	TR<	120	15.775	4.28	-	-	-	-	-	-
130	10.549	4.71	10.812	4.77	11.166	4.79	11.674	4.75	11.586	4.76	12.537	4.64	15.242	4.23	-	-	TR<	124	-	-	-	-	-	-
140	10.69	4.8	11.017	4.83	11.482	4.82	12.217	4.73	12.09	4.76	13.863	4.5	TR<	116	-	-	-	-	-	-	-	-	-	-
150	10.88	4.55	11.304	4.54	11.964	4.48	13.288	4.29	13.018	4.34	TR<	150	-	-	-	-	-	-	-	-	-	-	-	-
160	11.088	4.5	11.642	4.46	12.625	4.34	15.575	3.93	14.956	4.03	-	-	-	-	-	-	-	-	-	-	-	-	-	-
170	11.451	4.56	12.314	4.46	14.526	4.15	TR<	164	TR<	166	-	-	-	-	-	-	-	-	-	-	-	-	-	-
180	TR>	172	TR>	172	TR>	172	-	-	-	-	-	-	-	-	-	-	-	-	-	-	-	-	-	-

NOTE : a) KO = Temperature Difference Between Gas (TG) & Clad (TC)
b) Phot = Filling Gas Pressure at any Time During the Transient
c) Dmax = Maximum Tube Diameter at any Time During the Transient
d) Thermal History is as Shown in Table 1

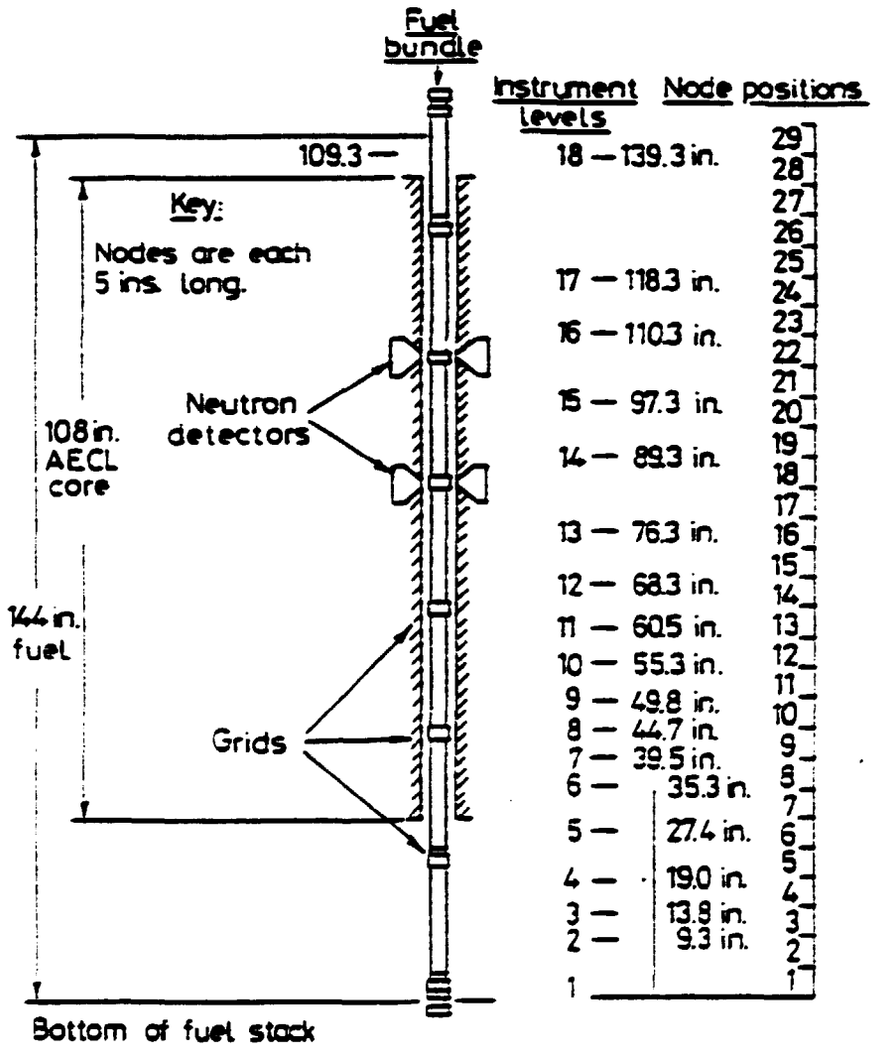

FIG.1. Schematic Illustration of NRU Fuel Bundle Rods.

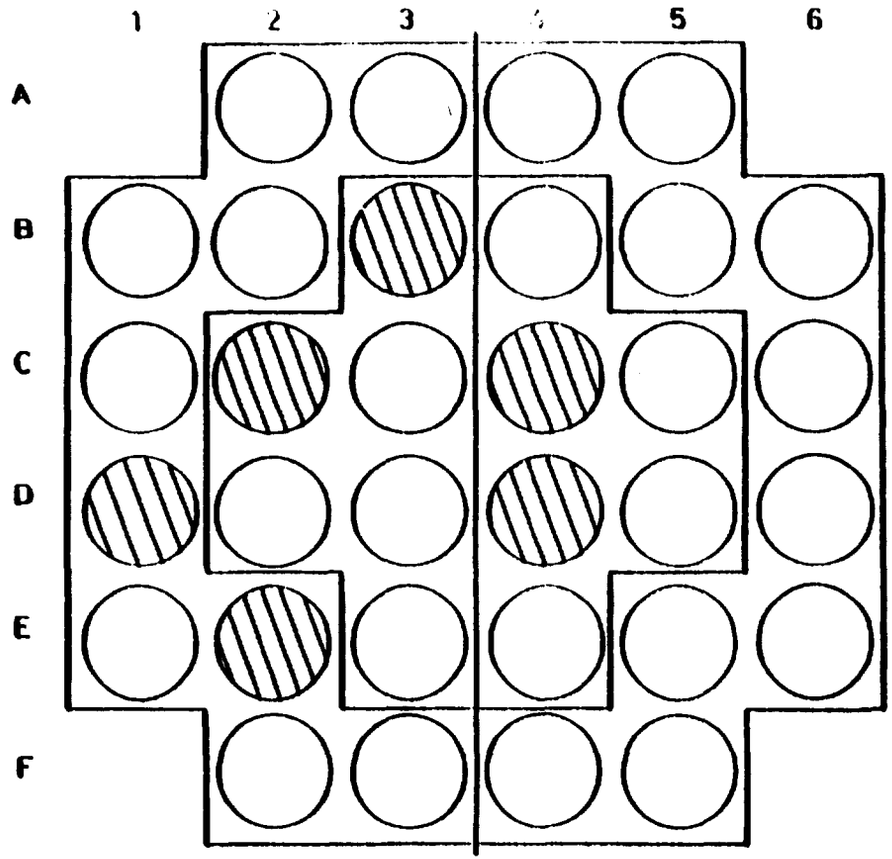

Rod number	Sensor ref. number	T/C level
2E	8	3
2E	24	8
2E	29	9
1D	39	11
3B	47	13
3B	61	15
4C	83	17
2C	115	18
4D	77	Plenum 19

FIG.2. Cross-Section of NRU Test Bundle; Thermocouples in Shaded Rods have been used to Construct an Axial Temperature Profile for Test TH-2.14.

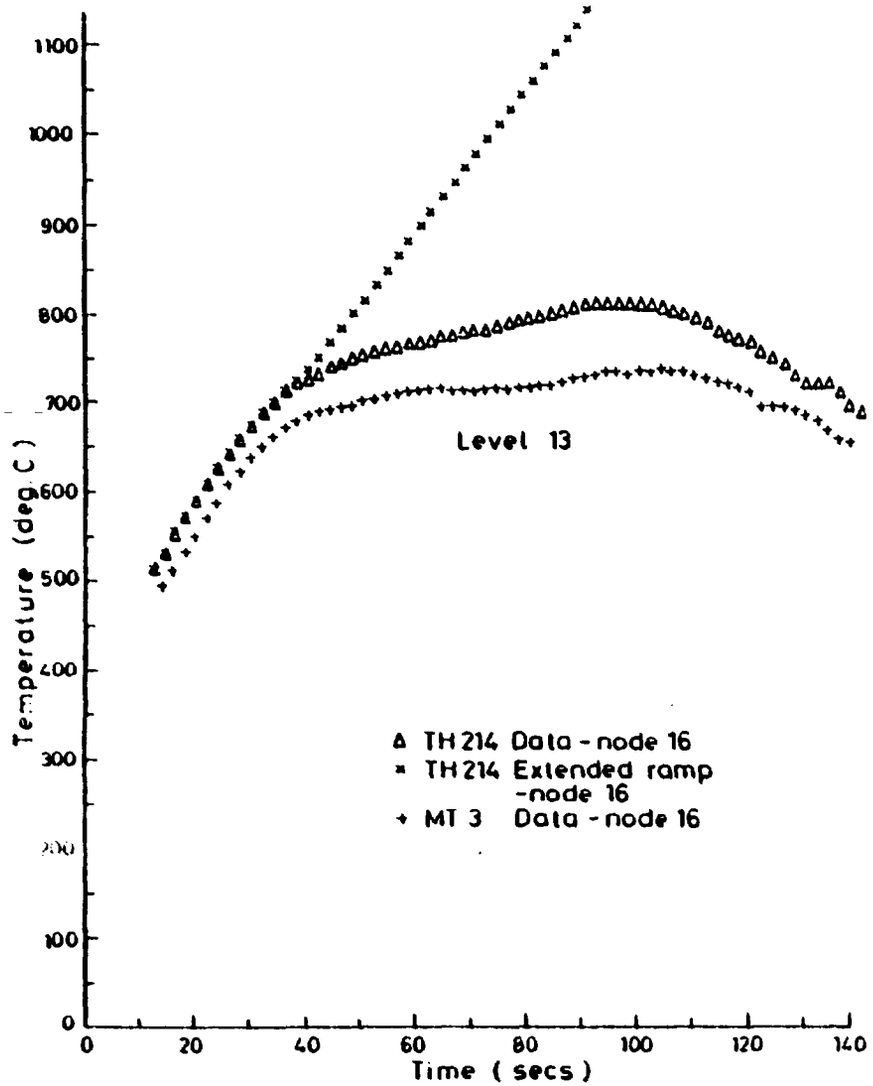

FIG.3. Temperature vs. Time Profiles at Axial Level 13 in Tests MT-3 & TH 2.14.

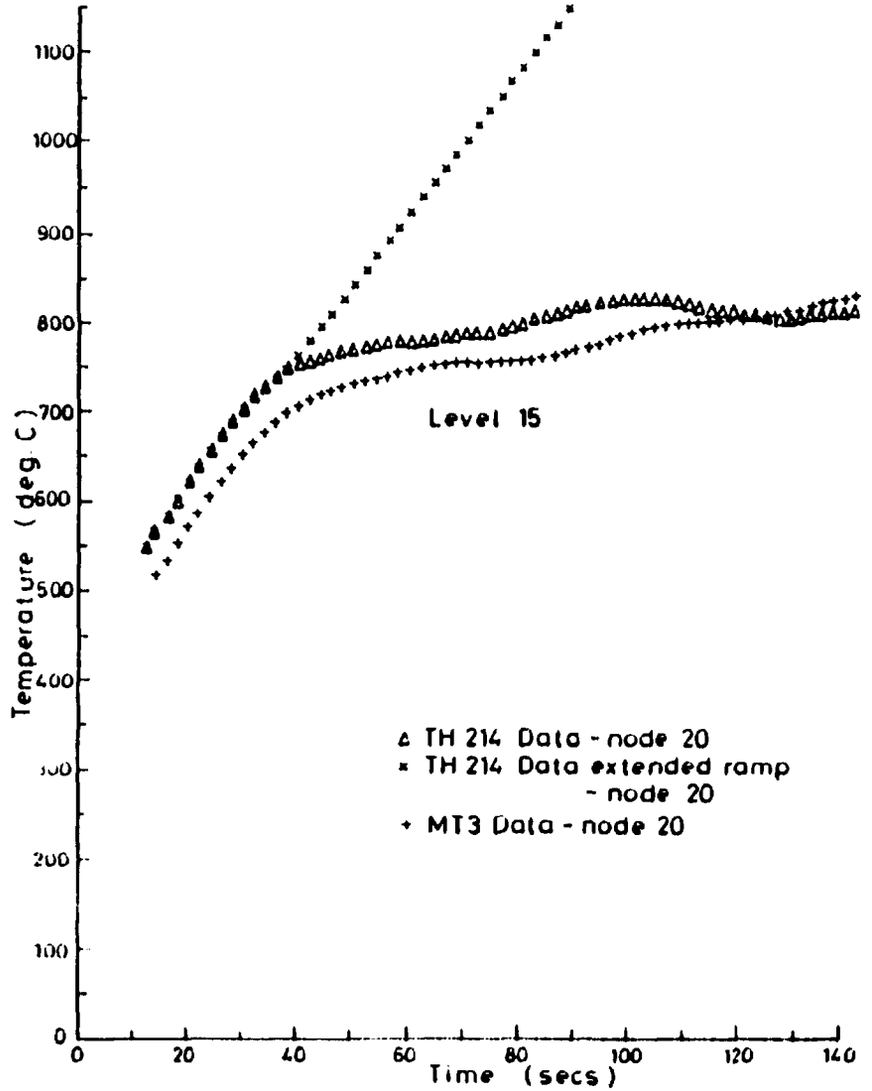

FIG.4. Temperature vs. Time Profiles at Axial Level 15 in Tests MT-3 & TH-2.14.

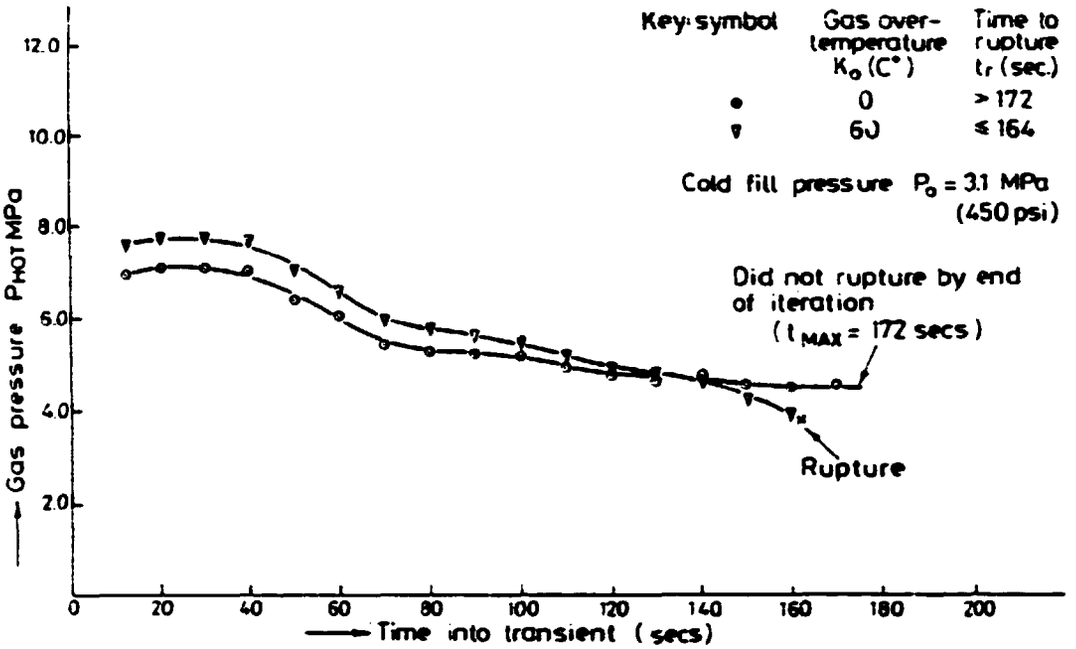

FIG.5a. Variation of Internal Gas Pressure, P_{HOT}, with Time during a Ballooning Transient for an Initial Cold Fill Pressure, P_o, of 3.1 MPa.

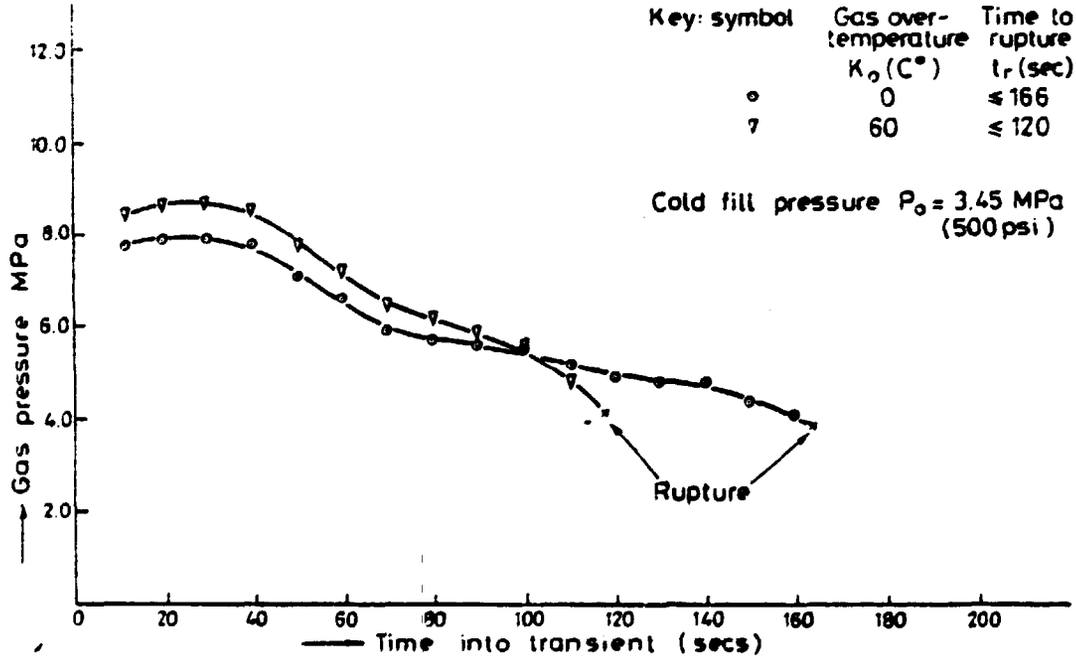

FIG.5b. Variation of Internal Gas Pressure, P_{HOT}, with Time during a Ballooning Transient for an Initial Cold Fill Pressure P_o of 3.45 MPa.

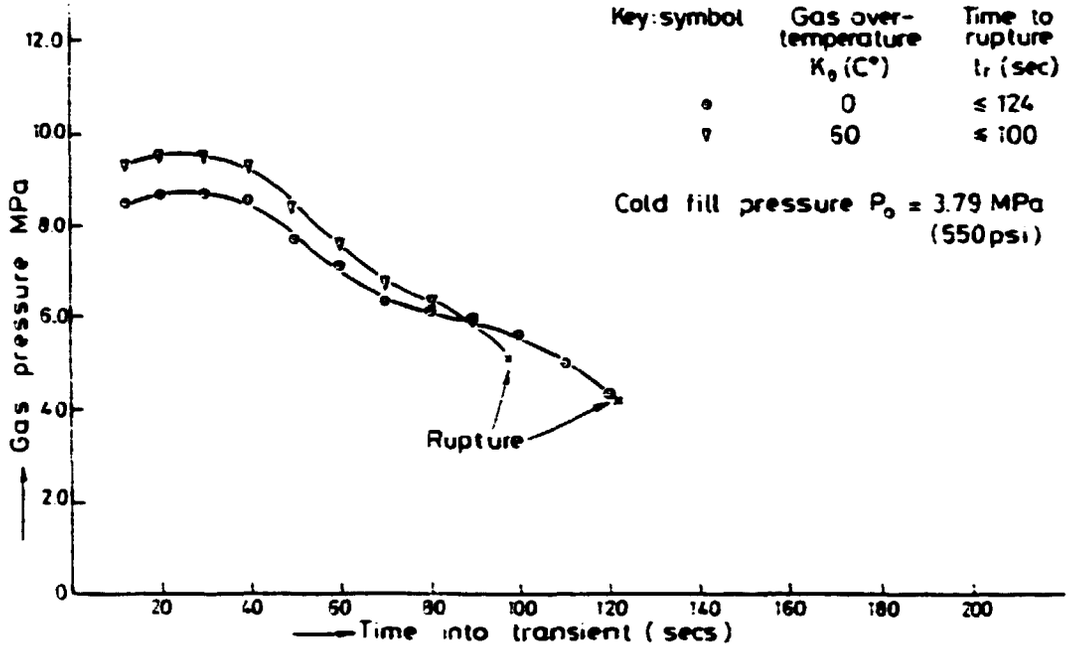

FIG.5c. Variation of Internal Gas Pressure, P_{HOT}, with Time during a Ballooning Transient for an Initial Cold Fill Pressure, P_o, of 3.79 MPa.

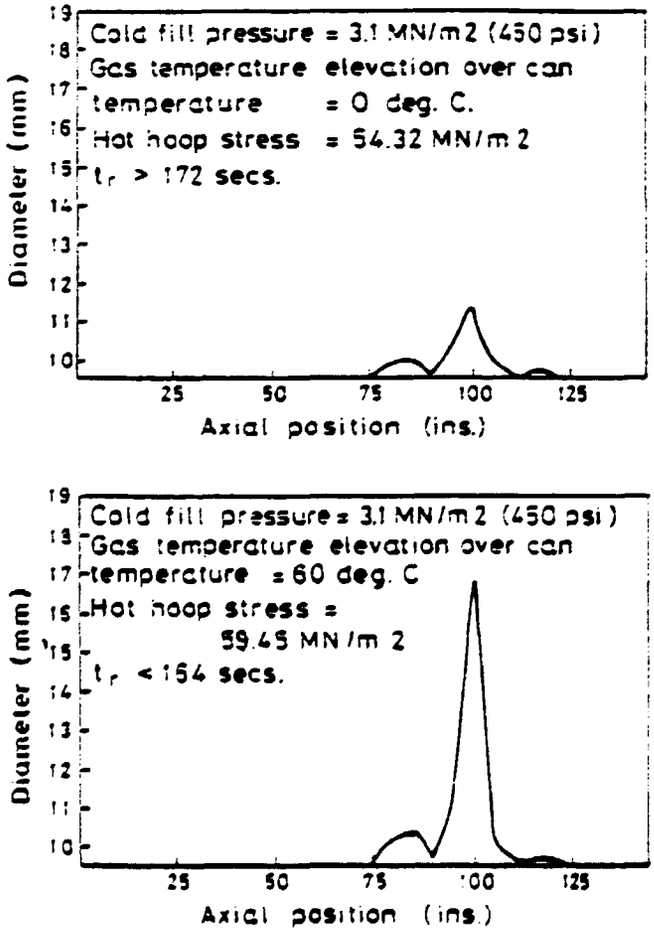

FIG. 6.

Variation of Calculated Rod Diameter as a Function of Axial Location.
(Thermal History as in Table 2.)

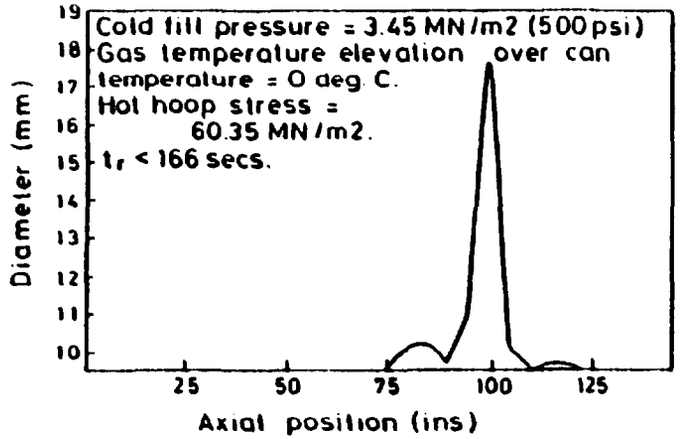

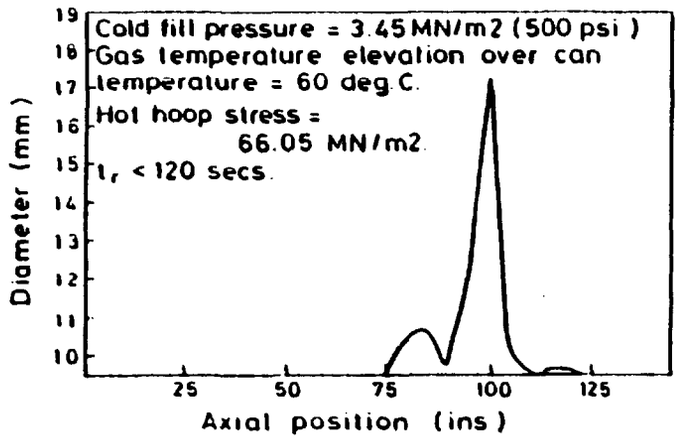

FIG. 7 Variation of Calculated Rod Diameter as a Function of Axial Location.
(Thermal History as in Table 2.)

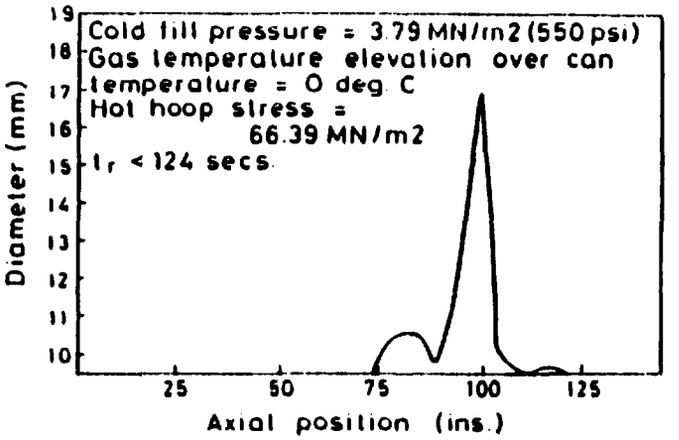

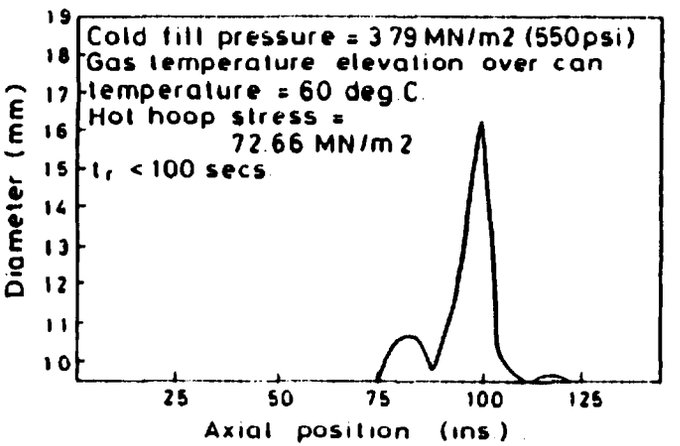

FIG. 8 Variation of Calculated Rod Diameter as a Function of Axial Location.
(Thermal History as in Table 2.)

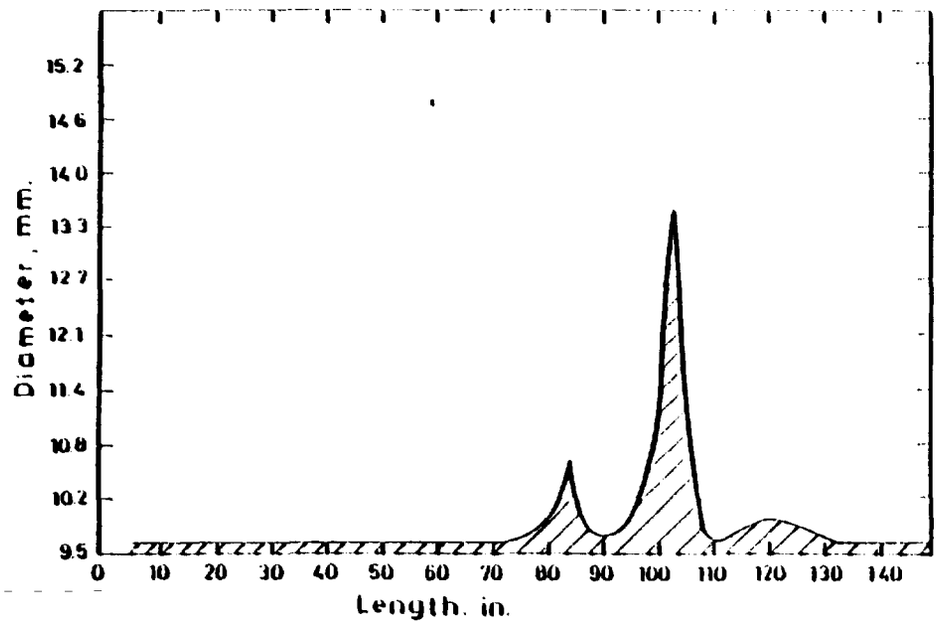

FIG. 9. Average Diametral Measurement versus Axial Elevation for a Typical Fuel Rod in Test MT-3.

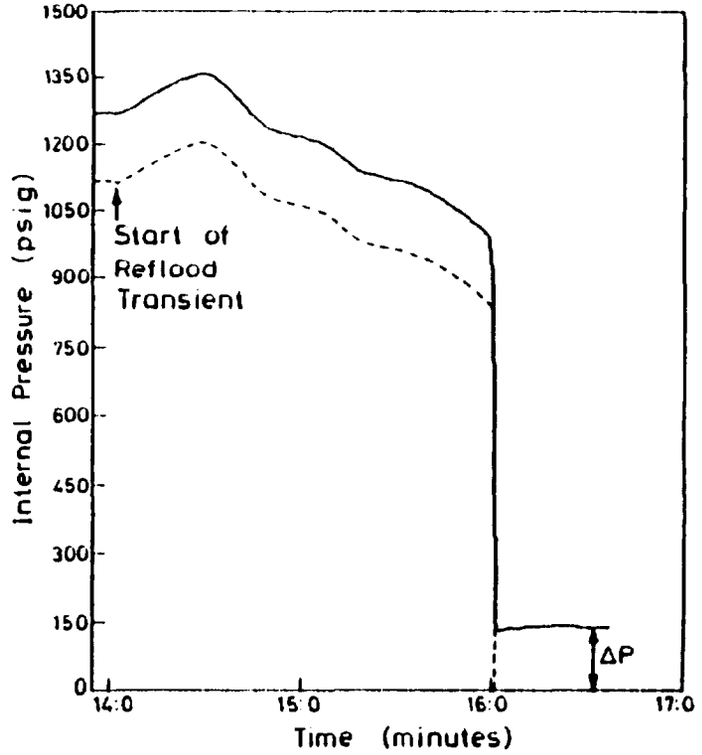

FIG. 10. Measured Variation of the Internal Pressure of Rod During Ballooning